ELSEVIER

Journal of Molecular Structure 525 (2000) 173–183

Journal of
MOLECULAR
STRUCTURE

www.elsevier.nl/locate/molstruc

Comparative study of the metal–ligand bond strength in Mn^{II}/X/U complexes (X = Cl, Br, I; U = urea)

R. Keuleers[a], G.S. Papaefstathiou[b], C.P. Raptopoulou[c], S.P. Perlepes[1,b], H.O. Desseyn[a,*]

[a]*Department of Chemistry, University of Antwerp—RUCA, Groenenborgerlaan 171, 2020 Antwerp, Belgium*
[b]*Department of Chemistry, University of Patras, 265 00 Patras, Greece*
[c]*Institute of Materials Science, NCSR "Demokritos", 153 10 Aghia Paraskevi Attikis, Greece*

Received 13 September 1999; received in revised form 20 December 1999; accepted 20 December 1999

Abstract

The synthesis, structure, vibrational analysis and a comparative vibrational study in function of the structure and the metal–ligand bond strength are discussed for a series of Mn(II)–urea–halogenide complexes. Complex $[MnCl_2U]$ has been prepared and studied for the first time. The single-crystal X-ray structure of the 1:6-bromide complex reveals the presence of octahedral $[MnU_6]^{2+}$ ions and bromide counterions.

Keywords: Halogeno manganese(II) complexes; Urea complexes; X-ray structure; Vibrational spectroscopy; Metal–ligand bond strength

1. Introduction

Although urea, H_2NCONH_2, is an old ligand, its coordination chemistry is currently an area of great activity, research in this area ranging from bioinorganic [1,2] to pharmaceutical [3,4] and material chemistry [5].

High-spin manganese(II) complexes are characterised by the absence of ligand field stabilisation energy, and this has two main consequences [6]: (i) a lower stability of manganese(II) complexes compared with those of other divalent metals of the first transition series and (ii) the possibility to obtain various coordination geometries. The manganese(II)–halide adducts are interesting because they show a variety of stoichiometries and geometries closely dependent on many factors, among which are interactions due to crystal packing and hydrogen bonding forces, halide dimensions as well as ligands' steric and electronic effects.

We report here an amalgamation of the above two topics, namely the preparation and characterisation of the complexes formed from the reactions between manganese(II) halides and urea (U). The characterisation involves the vibrational analysis of the complexes and the single-crystal X-ray structure of the complex $[MnU_6]Br_2$. Furthermore results from IR, far-IR and Raman measurements will be combined to obtain relevant information about the relative metal–ligand bond strengths. Brief comparisons with results from thermal measurements will also be made; the thermal characterisation of the prepared compounds will be reported elsewhere [7].

Literature contains limited information on MnX_2/U complexes. Compounds of the general formulae MnX_2U_m ($m = 2$, 4 for X = Cl; $m = 2$, 4, 6, 10 for

* Corresponding author. Tel.: + 32-3-2180365; fax: + 32-3-2180233.

E-mail addresses: perlepes@patreas.upatras.gr (S.P. Perlepes), keuleers@ruca.ua.ac.be (H.O. Desseyn).

[1] Tel.: + 30-61-997146; fax: + 30-61-997118.

0022-2860/00/$ - see front matter
PII: S0022-2860(00)00408-7

X = Br, $m = 6, 10$ for X = I) and $MnCl_2U(H_2O)_3$ have been isolated and partially studied [8–12]. Only the single-crystal X-ray structure of $[MnCl_2U_2]$ has been determined [13,14]. These studies focussed mainly on the determination of the coordination sphere of the complexes, but a thorough structural, vibrational, thermal and comparative study of Mn^{II}/X/U (X = Cl, Br, I) complexes has not been published yet.

2. Experimental

2.1. General

For the IR spectra 100 scans were recorded and averaged on a Bruker IFS 113v Fourier Transform spectrometer, using a liquid nitrogen cooled MCT detector with a resolution of 1 cm^{-1}. For the far-IR spectra 250 scans were recorded and averaged using a DTGS-detector with a resolution of 4 cm^{-1}. For the Raman spectra 1000 scans were recorded and averaged with a resolution of 4 cm^{-1} on a Bruker IFS 66v interferometer equipped with a FT Raman FRA106 module and a Nd–YAG laser. The thermogravimetric analysis experiments and the calorimetric measurements were performed on the SDT-2960 and on the DSC-2920 modules, respectively, from TA-instruments. A sample mass of approximately 15 mg was heated at a heating rate of 5°C/min in a N_2-atmosphere at a flow rate of 50 ml/min.

C, H and N were determined with a Carlo Erba 1106 analyser. Mn was determined using standard titrimetric procedures. Urea (U) and the metal salts were purchased from Aldrich with a purity higher than 99%.

2.2. Compound preparation

[$MnCl_2U$] was prepared by refluxing an ethanolic solution containing urea, an excess (3:1) of anhydrous $MnCl_2$ and 2,2-dimethoxypropane until a pale pink solid precipitated. The yield was larger than 80% based on urea. *Anal.* found (calcd): Mn: 29.51 (29.55); H: 2.10 (2.17); C: 6.43 (6.46); N: 15.00 (15.07).

[$MnCl_2U_2$] was prepared in the same way as $[MnCl_2U]$. Only stoichiometric amounts of $MnCl_2$ and urea were taken. This pale pink microcrystalline solid could also be obtained by slow evaporation of an ethanol solution with stoichiometric amounts of $MnCl_2$ and urea. Typical yields are in the 70–80% range. *Anal.* found (calcd): Mn: 22.20 (22.30); H: 3.18 (3.28); C: 10.02 (9.77); N: 22.90 (22.78).

[$MnCl_2U_4$] was obtained by stirring an ethanolic solution with stoichiometric amounts of $MnCl_2$, urea and 2,2-dimethoxypropane at room temperature. After half an hour Et_2O was added till a white solid precipitated. Stirring of this solution with an excess of urea (up to 1:20) yielded always the same product. $[MnU_6]Cl_2$ could not be isolated. The yield was approximately 50%. *Anal.* found (calcd): Mn: 15.00 (14.99); H: 4.35 (4.41); C: 13.19 (13.12); N: 30.56 (30.61).

[$MnBr_2U_2$] was obtained by slow evaporation of an ethanolic solution with stoichiometric amounts of $MnBr_2$ and urea until a pale brown solid precipitated. Refluxing, stirring or slow evaporation experiments with an excess of $MnBr_2$ never yielded the $[MnBr_2U]$-complex so that this compound could not be obtained. The yield was 70–80%. *Anal.* found (calcd): Mn: 16.35 (16.41); H: 2.37 (2.41); C: 7.22 (7.17); N: 16.67 (16.73).

[$MnBr_2U_4$] was prepared by refluxing an ethanolic solution of urea, a stoichiometric amount of $MnBr_2$ and 2,2-dimethoxypropane until a brown oil appeared. This oil was treated with Et_2O till a pale brown solid was obtained. This pale brown solid could also be isolated by slow evaporation of an ethanolic solution with stoichiometric amounts of $MnBr_2$ and urea. The yield was approximately 60%. *Anal.* found (calcd): Mn: 12.01 (12.08); H: 3.65 (3.54); C: 10.93 (10.56); N: 26.50 (24.63).

[MnU_6]Br_2 and *[MnU_6]I_2* were prepared by stirring stoichiometric quantities of urea and the metal salt in an ethanolic solution with a small amount of 2,2-dimethoxypropane at room temperature. After half an hour Et_2O was added till a white solid precipitated. Layering of the mother solution with an equal volume of Et_2O gave colourless crystals suitable for X-ray structural analysis. Refluxing, stirring or slow evaporation of an ethanol solution of MnI_2 and urea with lower stoichiometries than 1–6 always yielded the same product so that the $[MnI_2U]$, $[MnI_2U_2]$ and $[MnI_2U_4]$ complexes could not be prepared. The yield was approximately 30%. *Anal.* found (calcd): *Br:* Mn: 9.37 (9.54); H: 4.19 (4.21); C: 12.63 (12.53); N: 29.32 (29.23) *I:* Mn: 8.17 (8.20); H: 3.62 (3.62); C: 10.94 (10.77); N: 25.41 (24.12).

Table 1
Crystallographic data for complex $[MnU_6]Br_2$

Parameter	$[MnU_6]Br_2$
Empirical formula	$C_6H_{24}Br_2MnN_{12}O_6$
Formula weight	575.13
Space group	$P2_1/c$
Temperature (°C)	25
λ (Å)	0.71073
a (Å)	10.086 (7)
b (Å)	7.748 (6)
c (Å)	13.15 (1)
β (degrees)	93.37 (2)
V (Å^3)	1025.8 (1)
Z	2
ρ_{obsd} (g cm^{-3})	1.84
ρ_{calc} (g cm^{-3})	1.862
μ(Mo,Kα) (mm^{-1})	4.588
$R1$[a]	0.0190
$wR2$[a]	0.0557

[a] $w = 1/[\sigma^2(F_o^2) + (aP)^2 + bP]$ and $P = (\max(F_o^2, 0) + 2F_c^2)/3]$; $a = 0.0000$, $b = 0.1745$. $R1 = \sum(|F_o| - |F_c|)/\sum(|F_o|)$, $wR2 = \{\sum[w(F_o^2 - F_c^2)^2]/\sum(F_o^2)^2]\}^{1/2}$ for 1875 reflections with $I > 2\sigma(I)$.

All solids were collected by filtration, washed with Et_2O and dried in vacuo at room temperature. The deuterated complexes were prepared by dissolving the products in CH_3OD and evaporating the solution in vacuo. This procedure was repeated three times.

2.3. X-ray structure determination of $[MnU_6]Br_2$

A colourless prismatic crystal with approximate dimensions $0.20 \times 0.30 \times 0.50$ mm^3 was mounted in air. Diffraction measurements were made on a Crystal Logic Dual Goniometer diffractometer. Complete crystal data and parameters for data collection for the $[MnU_6]Br_2$ complex are reported in Table 1.

Unit cell dimensions were determined and refined by using the angular settings of 25 automatically centred reflections in the range $1 < 2\theta < 23°$. Intensity data were recorded using a θ–2θ scan to $2\theta_{max} = 52°$. Three standard reflections monitored every 97 reflections showed less than 3% fluctuation and no decay. Lorentz, polarisation and ψ scan absorption corrections were applied using Crystal Logic software. Symmetry equivalent data were averaged with $R = 0.0091$ to give 2013 independent reflections from a total of 2108 collected. The structure was solved by direct methods using SHELXS-86 [15] and refined by full-matrix least-squares techniques on F^2 with SHELXL-93 [16]. All non-hydrogen atoms were refined with anisotropic thermal parameters. All hydrogen atoms were located by difference maps and refined isotropically. The maximum and minimum residual peaks in the final difference map were 0.299 and -0.211 eÅ^{-3}.

3. Results and discussion

3.1. Structure of the Mn–urea–halogenide complexes

For all these complexes the Mn-atom has an octahedral surrounding (Fig. 1) and urea is coordinated to the metal by the oxygen atom. In the 1:6-complex, the halogens act as counterions in contrast with the 1:4-complex where they are bound directly to the metal in a *trans* position, and with the 1:2- and 1:1-complexes where they are bridged between different metal atoms.

From the seven complexes reported in Section 2, six have been isolated and partially characterised by other research groups in the past [8–10]. Structural assignments for these compounds were made by employing IR and far-IR (coordination mode of U, presence of X^- in the coordination sphere), UV/VIS (octahedral or tetrahedral geometry), EPR (covalent character in bonding, distortion of the coordination sphere, symmetry), X-ray powder diffraction (mutual isomorphism, isomorphism with complexes of known structures) and variable-temperature magnetic susceptibility measurements (high-spin character, possible magnetic interactions). Based on the above techniques the structural formulae shown in Fig. 1 were proposed [8,9]. Later the chloro-bridged chain structure of $[MnCl_2U_2]$ was confirmed by single-crystal X-ray crystallography [13,14]. Moreover the molecular and crystal structure of $[MnU_6]Br_2$ will be described below.

The $[MnCl_2U]$-complex has, to our knowledge, not yet been mentioned in the literature. We performed many crystallisation experiments, working mainly with DMF and DMSO, on this compound and on all the other compounds mentioned above, but we did not succeed, except for $[MnU_6]Br_2$, in preparing suitable crystals (twinning problems or lack of single crystals) for structure determination by X-ray diffraction. The structure of the 1:1-chloride complex has consequently

been determined by comparing the IR spectra (4000–500 cm^{-1}) of this compound and of $[CdCl_2U]$ for which the single-crystal X-ray structure has already been described in the literature [17,18]. As these two spectra have an identical profile we can assume that $[MnCl_2U]$ has a similar structure as given in Fig. 1. This polymeric structure involves μ_3-chloro ligands and monodentate O-bonded urea molecules. All these structures are confirmed by our vibrational analysis as will be described further in this article.

$[MnU_6]Cl_2$ could not be prepared probably because of the size of the chloride counterion which is too small to stabilise the big $[MnU_6]^{2+}$-ion in contrast with the bigger bromide and iodide ions (symbiotic effect). Thermal decomposition experiments on the $[MnU_6]I_2$-complex always yielded complexes in which the CO- and NH-bonds in the ligand were broken, with the formation of nitriles, of which the vibrational bands are clearly visible in the infrared spectrum, as a consequence, in contrast with the chloride and the bromide complexes in which compounds with a lower Mn–urea stoichiometry were formed according to the following scheme [7]:

$$[MnU_6]X_2 \rightarrow [MnX_2U_4] \rightarrow [MnX_2U_2] \rightarrow [MnX_2U] \rightarrow MnX_2$$

Consequently we could not obtain, not in the laboratory nor by thermal analysis, any urea complex in which the iodide was bound directly to the metal. This is probably due to the fact that, according to the HSAB-theory [19], the iodide is too soft to bind directly to the hard manganese ion in competition with the hard oxygen atoms of the urea ligands. The bromine atom is probably also too soft to be bridged between three hard Mn-atoms explaining why the $[MnBr_2U]$ complex could not be isolated.

3.2. X-ray structure of $[MnU_6]Br_2$

An ORTEP plot of the cation of the $[MnU_6]Br_2$ complex is shown in Fig. 2. Selected interatomic distances and angles are listed in Table 2.

The structure consists of the octahedral $[MnU_6]^{2+}$ cation and of bromide counterions, and is stabilised through a complex scheme of inter- and intramolecular hydrogen bonds involving all the urea

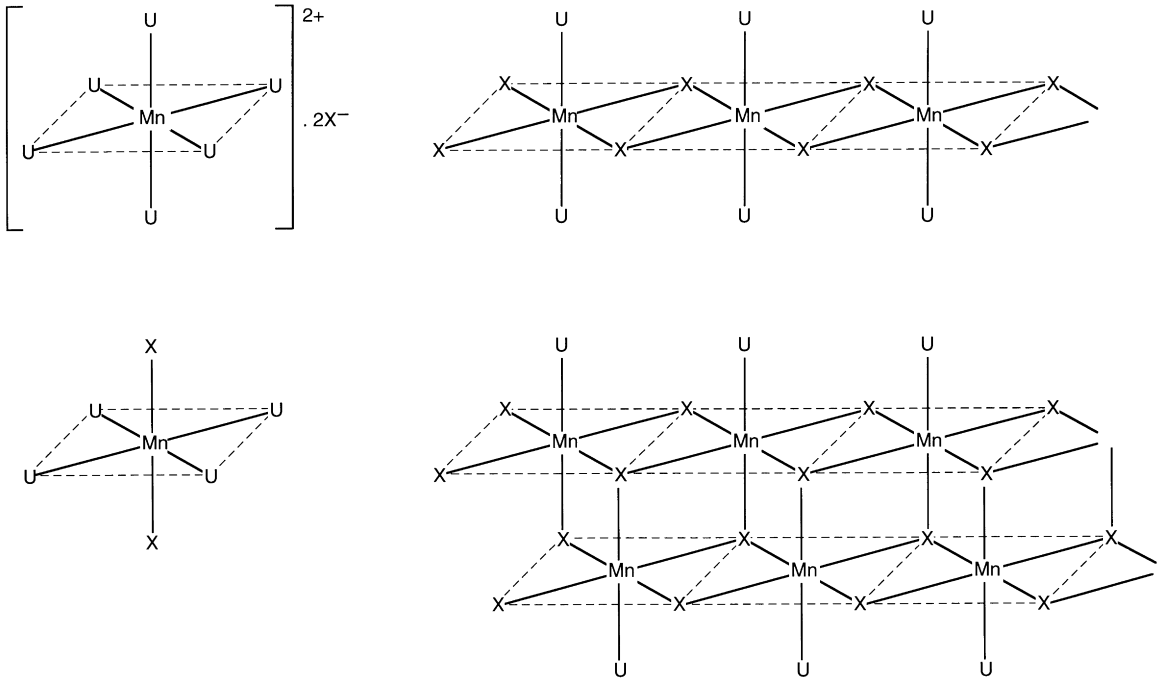

Fig. 1. Structure of MnU_6X_2 (top left), MnU_4X_2 (bottom left), MnU_2X_2 (top right) and $MnUX_2$ (bottom right).

Table 2
Selected interatomic distances (Å) and angles (°) for complex $[MnU_6]Br_2$

Distances				
Mn–O(1)	2.181 (2)	O(1)–C(1)	1.259 (2)	
Mn–O(11)	2.192 (2)	C(1)–N(1)	1.321 (3)	
Mn–O(21)	2.199 (2)	C(1)–N(2)	1.332 (3)	
Angles				
O(1)–Mn–O(11)	87.9 (1)	Mn–O(1)–C(1)	135.1 (1)	
O(1)–Mn–O(21)	87.5 (1)	Mn–O(11)–C(11)	138.9 (1)	
O(11)–Mn–O(21)	89.0 (1)	Mn–O(21)–C(21)	129.0 (1)	
Hydrogen bonds[a,b]				
D	H	A	D···A (Å)	D–H···A (degrees)
N(1)	H(N(1A))	O(21)[i]	2.895	159.4
N(11)	H(N(11B))	O(1)[i]	3.119	145.6
N(21)	H(N(21B))	O(1)[ii]	3.092	128.0
N(12)	H(N(12A))	O(11)[iii]	2.947	175.7
N(22)	H(N(22A))	O(21)[iv]	3.226	134.6
N(1)	H(N(1B))	Br[ii]	3.581	159.6
N(11)	H(N(11A))	Br[v]	3.547	156.8
N(21)	H(N(21A))	Br[vi]	3.433	168.2
N(2)	H(N(2A))	Br[vii]	3.608	175.7
N(2)	H(N(2B))	Br[ii]	3.681	157.2
N(12)	H(N(12B))	Br[v]	3.523	153.7
N(22)	H(N(22B))	Br[vi]	3.834	136.5

[a] Symmetry operations: (i) $1-x,-y,1-z$; (ii) x,y,z; (iii) $1-x,1-y,1-z$; (iv) $1-x,-0.5+y,0.5-z$; (v)$1-x,0.5+y,1.5-z$; (vi) $-x,-y,1-z$; (vii) $x,0.5-y,-0.5+z$.
[b] A = Acceptor, D = Donor.

nitrogen and oxygen atoms, and all the bromide counterions. The Mn(II) atom is located on an inversion centre. The octahedron is slightly distorted around the metal ion with O–Mn–O angles ranging from 87.5 (6) to 92.5 (6)°. The average Mn–O distance is 2.19 Å, as in other octahedral manganese(II) complexes with O-donors [20]. The coordination mode of the urea molecules is classical (monodentate and angular) with Mn–O–C angles ranging from 129.0 (1) to 138.9 (1)° as in most complexes of urea and its derivatives [21]. $[MnU_6]Br_2$ joins a handful of structurally characterised manganese(II) complexes of urea [13,14,22,23].

3.3. Vibrational analysis of the Mn(II)–urea–halogenide complexes

As we have already mentioned, literature on the vibrational analysis of these complexes is poor. Barbier [8] and Antonenko [10] decided on a metal–oxygen coordination out of the shifts of the bands of the νCO and the νCN on complexation. Barbier [9] also tried to assign the far-IR spectra by comparing the spectra of these compounds with analogue complexes but had to restrict himself to the Mn–O and Mn–X stretching vibrations due to the complex pattern of the spectra. We solved the vibrational spectrum of these compounds by using our knowledge of the free ligand [24–26] and by comparing the spectra of the normal and the deuterated complexes. The results of our vibrational analysis are given in Table 3.

In the νNH_2 region we clearly see the νNH_2 bands shifting to higher wavenumbers on complexation, indicating weaker hydrogen bonds compared with the free ligand. In urea hydrogen bonds are formed with the oxygen atom of the urea molecule, but because of the metal–oxygen coordination in the complexes this atom becomes less available and thus weaker hydrogen bonds could be expected. We also see a bigger shift of these bands to higher wavenumber for the polymeric structures ($[MnX_2U]$, $[MnX_2U_2]$) than for the 1:4- and the 1:6-coordinations. This is probably due to sterical reasons: as

Table 3
Vibrational analysis of the Mn(II)–urea–halogenide complexes

	Urea	$[MnCl_2U]$	$[MnCl_2U_2]$	$[MnCl_2U_4]$	$[MnBr_2U_2]$	$[MnBr_2U_4]$	$[MnU_6]Br_2$	$[MnU_6]I_2$
νNH_2	3450–3331	3476–3357	3476–3340	3479–3364	3476–3364	3476–3340	3475–3378	3480–3375
$\delta_s NH_2 + \nu C{-}O$	1683	1676	1664	1656	1656	1654	1665	1657
$\delta_{as} NH_2$	1625	1634	1632	1642	1629	1639	1640	1637
$\nu C{-}O + \delta_s NH_2$	1601	1590	1583	1583	1580	1588	1575	1570
$\nu_{as} C{-}N$	1466	1487	1477	1475	1480–1475	1494–1480	1476	1473
$\rho_s NH_2$	1153	1153	1151	1153	1146	1156	1170	1165
$\rho_{as} NH_2$	1057	1079	1082	1071	1072	1048	1043	1047
$\nu_s C \not\succ N$	1003	1023	1018	1016	1018	1018	1016	1014
$\pi C{-}O$	789	760	775	778	775	775	773	770
$\tau_{as} NH_2$	727	650	678	667	671	693	688	676
$\delta C{-}O$	569	603	598	598	593	594	604	599
$\delta C{-}N$	530	539	534	525	532	537	536	536
$\omega_{as} NH_2$	508	499	495	493	488	487	500	500

the halogens are bridged between several metal atoms in the polymeric structures (Fig. 1), they are less available for hydrogen atoms than when they are bound to only one metal ($[MnX_2U_4]$) or act as counterions ($[MnU_6]X_2$) and can freely orient themselves in function of hydrogen bonding.

For the free ligand we observed and calculated for the normal and for the deuterated compound an

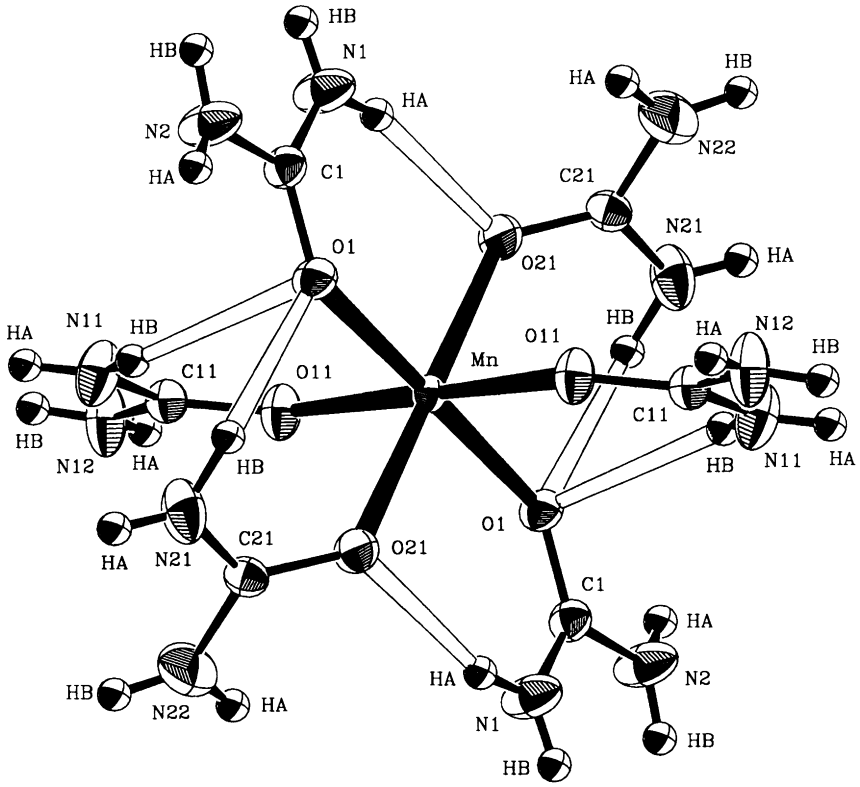

Fig. 2. ORTEP plot of $[MnU_6]Br_2$.

intensive coupling of the νCO with the $\delta_s NH_2$-mode and the ν_sCN-mode, respectively [24–26]. As we observe similar profiles and intensity changes on deuteration for both the free ligand and the complex-ligand we can assume comparable PED-values: on deuteration we clearly see the two intense IR bands and the two medium intense Raman peaks between 1630 and 1680 cm^{-1} disappear, indicating δNH_2 character, and the intense IR band and weak Raman peak between 1570 and 1590 cm^{-1}, assigned to the νCO vibration, shift to higher wavenumber. This clearly indicates, as in the free ligand [24–26], a coupling between the νCO and the $\delta_s NH_2$ vibrations. As the νCO is not a pure vibration it cannot be used for comparative studies as we will demonstrate further in this article.

In normal urea the ν_sCN is a pure vibration but after deuteration an intense coupling with the $\rho_s ND_2$ vibration appeared, which was clearly visible on the relative intensity changes of the corresponding bands in the IR and in the Raman spectrum [25]. A similar intensity change is visible in the IR and in the Raman spectra of the complexes. In the Raman spectrum of $[MnU_6]I_2$ the two ρNH_2 and the ν_sCN vibrations are assigned to the weak bands at 1165 and 1047 cm^{-1} and to the very intense band at 1014 cm^{-1}, respectively. On deuteration we clearly see these two weak and one very intense band changing into two medium intense bands at 1002 and 902 cm^{-1} and one shoulder at 887 cm^{-1}. This relative intensity change points out, as in the free ligand, a coupling between the ν_sCN and the($\rho_s ND_2$ vibrations. The same relative intensity changes are observed in the IR spectrum of $[MnU_6]I_2$.

The weak, broad signals around 675 and 495 cm^{-1} disappear on deuteration and are consequently assigned to the $\tau_{as}NH_2$ and the $\omega_{as}NH_2$ vibrations. These pure vibrations shift to lower frequency on complexation confirming the weaker hydrogen bonds in the complexes compared with the free ligand.

The shifts of the two νC–N to higher and of the πC–O to lower frequency on complexation are indicative for a metal–oxygen coordination [27].

The weak, broad Raman band at 290 cm^{-1} and the shoulder on the high frequency side of the intense far-IR band at 247 cm^{-1}in the $[MnCl_2U]$ spectra are assigned to the metal–oxygen stretching vibration. Further assignments of these spectra are difficult because of the large number of bands and partial coinciding or coupling of these bands between them or with bands originating from lattice vibrations.

In the spectra of the 1:2-complexes the intense IR band at 272 cm^{-1} and the weak Raman band at 222 cm^{-1} stay unaffected on halogen substitution and are consequently assigned to the metal-oxygen stretching vibration. The intense IR bands of the chloride complex at 216, 164 and 132 cm^{-1}, and the weak Raman peaks at 241, 162 and 135 cm^{-1}, shift under influence of the mass effect to lower frequency (IR: 201, 152, 128 cm^{-1}; Raman: 183, 150, 132 cm^{-1}) on substitution of the chloride through a bromide atom and are consequently assigned to the metal–halogen bending vibrations.

The intense band at 219 cm^{-1} in the far-IR spectrum of the 1:4-chloride complex shifts to lower frequency on halogen substitution and can consequently be assigned to the metal–halogen stretching vibration. As the shoulders at 234 and 213 cm^{-1} and the band at 184 cm^{-1} shift to higher wavenumber (249, 232 and 200 cm^{-1}) on halogen substitution of the chloride through a bromide atom, they are assigned to the metal–oxygen bending vibrations. The weak Raman bands at 241, 187 and 160 cm^{-1} in the chloride spectrum shift to higher wavenumber (259, 201, 160 cm^{-1}) on halogen substitution and are consequently assigned to the metal–oxygen stretching and bending vibrations, respectively. The weak band at 205 cm^{-1} in the chloride spectrum appears at lower frequency (175 cm^{-1}) in the bromide spectrum and is consequently assigned to the metal–halogen stretching vibration.

The intense far-IR bands at 240 and 165 cm^{-1} in the spectra of the 1:6-complexes are assigned to the metal–oxygen stretching and metal–oxygen bending vibrations, respectively. In these spectra there are also two weak absorptions visible at 265 and 200 cm^{-1} which probably originate from a splitting of the two intense absorptions at 240 and 165 cm^{-1} because of the small distortion of the octahedral surrounding of the manganese atom (see Section 3.2). The weak, broad Raman peaks at 250, 195 and 158 cm^{-1} are assigned to the two metal–oxygen stretching and the metal–oxygen bending vibrations, respectively. The broad character of these bands also indicates a small distortion of the octahedral surrounding of the

Table 4
Infrared and Raman frequencies of urea and the Mn–halogenide complexes (cm^{-1}), *deuterated complexes

	Urea		$[MnCl_2U_4]$		$[MnCl_2U_2]$		$[MnCl_2U]$		$[MnU_6]Br_2$		$[MnBr_2U_4]$		$[MnBr_2U_2]$		$[MnU_6]I_2$	
	IR	Raman	IR	Raman	IR	Raman	IR	Raman	IR	Raman	IR	Raman	IR	Raman	IR	Raman
ν_{as}C–N	1466	1466	1471	1470	1477	1478	1487	1503	1478	1477	1478–1494	1491	1473–1478	1478	1476	1477
ν_{s}C–N	1003	1010	1011	1017	1018	1018	1024	1026	1017	1018	1018	1023	1018	1018	1018	1018
πC–O	790	790	778	788	777	779	760	761	777	776	777	[a]	777	777	773	782
ν_{as}C–N*	1485	1485	1504	[a]	1509	[a]	1521	[a]	1501	[a]	1514	[a]	1507	[a]	1501	[a]
πC–O*	778	778	770	777	763	775	755	753	768	766	765	765	763	765	763	764

[a] Too weak to be observed.

manganese atom. The other bands visible in these spectra are assigned to lattice vibrations.

3.4. Comparative study of the metal–oxygen bond strength in the Mn–urea–halogenide complexes

For stronger metal–ligand bonds a lower CO- and higher CN-stretching frequencies, and a lower πCO-mode are expected [27].

From the νCN- and the πCO-frequencies of the chloride complexes in Table 4 we can conclude that the metal–oxygen bond is stronger for the 1:1- than for the 1:2- and the 1:4-complex. This tendency could not be concluded from the νCO frequency.

The band with pure νCO-character should be very diagnostic for the determination of the metal–ligand bond strength. However, for the free ligand [24–26] and for the complexes (see Section 3.3) we determined for the normal and for the deuterated compound an intensive coupling with the $\delta_s NH_2$-mode and with the ν_sCN-mode, respectively. On coordination we expect a lowering of the νCO- and an increased frequency for the $\delta_s NH_2$- and ν_sCN-modes. As these contributions have an opposite effect we cannot consider this fundamental in the determination of the metal–ligand bond strength. This is indeed confirmed by the experiments. For the ligand the band with the highest νCO-character is situated at 1601 cm^{-1}. This band shifts to lower frequency for all complexes indicating a metal–oxygen bond [27]. However the magnitude of the observed frequency shift is opposite to the expected values considering the relative metal–ligand bond strength: the band at 1601 cm^{-1} is shifted to 1590 cm^{-1} for the 1:1-, 1583 cm^{-1} for the 1:2- and 1573 cm^{-1} for the 1:4-complex. This opposite effect must be due to the different amount of coupling of the νCO- and the $\delta_s NH_2$-vibrations in these complexes. A similar effect is observed for the deuterated complexes. For these reasons the CO-stretching vibration will not be used in further discussion. Frequencies corresponding to metal–oxygen stretching vibrations cannot be used to compare these compounds because of their different structural symmetry.

Thermal stabilities from TGA-measurements and ΔH-values from DSC-measurements confirm the proposed relative metal–oxygen bond strength: the 1:1-complex is the thermally most stable compound and needs the most energy to break one metal–urea bond (132 vs. 110 and 58 kJ/mol for the 1:2- and the 1:4-complexes) [7].

This relative metal–oxygen bond strength can be explained by comparing the structure of these complexes (Fig. 1): as the number of bridged halogen atoms increases from the 1:4- to the 1:2- and the 1:1-chloride complex, the electron density is concentrated more between the metal and the directly bonded urea molecules, with a stronger metal–oxygen bond in the 1:1- than in the 1:2- and the 1:4-chloride complex as a consequence.

For the bromide complexes, vibrational shifts show (Table 4) that the metal–oxygen bond strengths are comparable for these compounds.

Again frequencies corresponding to metal–oxygen stretching vibrations are not considered because of the different structural symmetries of these compounds.

Vibrational shifts also show (Table 4) a stronger metal–oxygen bond in the 1:4-bromide in comparison with the 1:4-chloride complex.

The same conclusion can also be drawn from the manganese–oxygen frequencies: as in the far-IR and in the Raman spectra the manganese–oxygen vibrations shift to higher wavenumber on halogen substitution of the chloride through a bromide atom, a stronger metal–oxygen bond can be considered for the 1:4-bromide complex.

TGA- and DSC-measurements also indicate a stronger metal–urea bond in the 1:4-bromide than in the 1:4-chloride complex confirming the results from the vibrational spectra: the 1:4-bromide complex is thermally more stable and needs more energy to break one metal–urea bond (80 vs. 58 kJ/mol) [7].

The difference in metal–oxygen bond strength can be explained by comparing the electronegativities of a chloride and a bromide atom. The chloride atom, which is more electronegative than the bromide atom, attracts the electrons from the metal relatively more, resulting in a lower electron density between the metal and urea, and consequently a weaker metal–oxygen bond.

Vibrational shifts also show (Table 4) that the metal–oxygen bond strength is comparable for the 1:2-complexes.

The same conclusion can also be drawn from the metal–oxygen vibrations: in the far-IR and in the Raman spectra the manganese–oxygen stretching

vibrations give rise to bands at 272 and 222 cm^{-1}, respectively, for both the chloride and the bromide complexes.

TGA- and DSC-measurements also indicate a similar metal–urea bond strength in the 1:2 complexes confirming the results from the vibrational spectra: the 1:2-complexes have the same thermally stability and need approximately the same energy to break one metal–urea bond (Cl: 110 kJ/mol; Br: 114 kJ/mol) [7].

Considering the electronegativity difference between a chloride and a bromide atom, one could expect a small difference in metal–oxygen bond strength as well. As the halogen atoms in the 1:2-complexes are bridged (Fig. 1), this influence is minimised probably because of the longer metal–halogen bond in the 1:2- compared to the 1:4-complex.

Vibrational shifts also indicate (Table 4) comparable metal–oxygen bond strengths for the 1:6-complexes.

As the far-IR and the Raman spectra of these compounds are also identical (see Section 3.3), a comparable metal–oxygen bond strength can be considered as well from the metal–oxygen frequencies.

The thermal stability of the two 1:6-complexes is also approximately the same confirming the results from the vibrational spectra. DSC-results of the 1:6-bromide and 1:6-iodide complex cannot be compared because the two complexes decompose in a different way [7].

As the halogen only occurs as a counterion in these 1:6-complexes (Fig. 1) and consequently exhibits no direct influence on the electron distribution around the metal, a comparable metal–oxygen bond could be expected.

4. Conclusion

In this article the synthesis, structure and vibrational analysis of the Mn(II)–urea–halogenide complexes were discussed. Furthermore a comparative study by vibrational spectroscopy of the metal–ligand bond strength in these complexes was also performed. Results from thermogravimetric analysis and calorimetric measurements were used to confirm the results of this comparative study. Complex $[MnCl_2U]$ has been prepared and studied for the first time. The single-crystal X-ray structure of the 1:6-bromide complex revealed the presence of octahedral $[MnU_6]^{2+}$ ion and bromide counterions.

Acknowledgements

R. Keuleers wishes to thank the FWO-V for a grant. The FWO-V is also acknowledged for the financial support towards the purchase of the thermal-analysis equipment. The authors also thank G. Thijs for technical assistance and J. Janssens for the TA-measurements.

References

[1] H.E. Wages, K.L. Taft, S.J. Lippard, Inorg. Chem. 23 (1993) 4985.
[2] T. Koga, H. Furutachi, T. Nakamura, N. Fukita, M. Ohba, K. Takahashi, H. Okawa, Inorg. Chem. 37 (1998) 989.
[3] A.I. Stetsenko, L.S. Tikhonova, M.A. Presnov, A.L. Konovalova, Dokl. Akad. Nauk. SSSR 243 (1978) 381.
[4] T. Theophanides, P.D. Harvey, Coord. Chem. Rev. 76 (1987) 237.
[5] M.D. Hollingsworth, K.D.M. Harris, in: J.L. Atwood, D.D. MacNicol, J.E.D. Davies, F. Vogtle, J.-M. Lehn (Eds.), Comprehensive Supramolecular Chemistry, Vol. 4, Pergamon, Oxford, 1996, pp. 177–223 chap. 7.
[6] B. Chiswell, E.D. McKenzie, L.F. Lindoy, in: G. Wilkinson, R.D. Gillard, J.A. McCleverty (Eds.), Comprehensive Coordination Chemistry, Vol. 4, Pergamon, Oxford, 1987, pp. 1–122 chap. 41.
[7] R. Keuleers, J. Janssens, H.O. Desseyn, Thermochima. Acta. (to be published).
[8] J.P. Barbier, R. Hugel, Inorg. Chim. Acta 10 (1974) 93.
[9] J.P. Barbier, R.P. Hugel, P.J. Van der Put, J. Reedijk, J. Roy. Neth. Chem. Soc. 95 (1976) 213.
[10] N.S. Antonenko, Y.A. Nuger, Zh. Neorg. Khim. 11 (1966) 1072.
[11] M.S. Lupin, G.E. Peters, Thermochim. Acta 73 (1984) 79.
[12] P.C. Srivastava, B.N. Singh, C. Aravindakshan, K.C. Banerji, Thermochim. Acta 71 (1983) 227.
[13] Y.Y. Kharitonov, T.N. Gushchina, E.B. Chuklanova, Koord. Khim. 12 (1986) 1145.
[14] Y.Y. Kharitonov, T.N. Gushchina, Zh. Neorg. Khim. USSR 32 (1987) 1848.
[15] G.M. Sheldrick, SHELXL86—Structure Solving, University of Gottingen, Germany, 1986.
[16] G.M. Sheldrick, SHELXL93—Program for Crystal Structure Refinement, University of Gottingen, Germany, 1993.
[17] M. Nardelli, A. Braibanti, I. Chierici, Gazz. Chim. Ital. 87 (1957) 1226.

[18] M. Nardelli, Gazz. Chim. Ital. 89 (1959) 1616.
[19] R.G. Pearson, J. Am. Chem. Soc. 85 (1963) 3533.
[20] J. Delaunay, R.P. Hugel, Inorg. Chem. 28 (1989) 2482.
[21] L. Lebioda, Acta Crystallogr. B 36 (1980) 271.
[22] G.V. Tsintsadze, T.I. Tsivtsivadze, F.V. Orbeladze, Zh. Strukt. Khim. 15 (1974) 306.
[23] M. Fujino, N. Achiwa, N. Koyano, I. Shibuya, Ridwan, K. Yamagata, J. Magn. Mater. 104 (1992) 851.
[24] B. Rousseau, R. Keuleers, H.O. Desseyn, C. Van Alsenoy, J. Phys. Chem. A 102 (1998) 6540.
[25] R. Keuleers, H.O. Desseyn, B. Rousseau, C. Van Alsenoy, J. Phys. Chem. A 103 (1999) 4621.
[26] B. Rousseau, R. Keuleers, H.O. Desseyn, H.J. Geise, C. Van Alsenoy, Chem. Phys. Lett. 302 (1999) 55.
[27] R.B. Penland, S. Mizushima, C. Curran, J.V. Quagliano, J. Am. Chem. Soc. 79 (1957) 1575.